Polymer Chemistry

ROYAL SOCIETY OF CHEMISTRY

PAPER

View Article Online
View Journal | View Issue

Cite this: *Polym. Chem.*, 2024, **15**, 3204

Anionic polymerization of phenyl-substituted isoprene derivatives: polymerization behaviour and cyclization-enabled fluorescence†

Moritz Rauschenbach,[a] Laura Stein,[a] Gregor M. Linden,[a] Ramona Barent,[a,b] Katja Heinze [a] and Holger Frey *[a]

1,3-Dienes are important monomers for living anionic polymerization. However, phenyl-substituted diene monomer structures have been rarely investigated. Based on DFT calculations and ^{13}C NMR spectroscopy, a discrepancy in the reactivity of the two monomers 1-phenyl isoprene (1PhI) and 4-phenyl isoprene (4PhI) in anionic polymerization is expected. Starting from a Wittig reaction including an optimized extraction procedure, disubstituted 1,3-dienes were obtained that resulted in polymers with different degrees of 1,3-incorporation. The polymers have been characterized by ^{1}H NMR spectroscopy and using different SEC conditions. Molecular weights of up to 48.8 kg mol^{-1} with narrow dispersities ($Đ \leq 1.13$) were achieved. The addition of the modifier THF led to an initial increase of vinyl units as well as a loss of control over the polymerization of 4PhI. Increasing the THF concentration further resulted in a rather unusual decrease of the vinyl units and ended with more than 80% 1,4-units in pure THF. Copolymerizations with styrene (S) and isoprene (I), respectively, were tracked *via in situ* ^{1}H NMR kinetics. The observed ideally random copolymerizations of I and 1PhI as well as the gradient copolymers with S were further investigated *via* the synthesis of copolymers with a targeted M_n of 40 kg mol^{-1}. In a subsequent reaction step, the homopolymers were cyclized using trifluoromethyl sulfonic acid inducing fluorescence properties. The different microstructures and substitution patterns of the original polymers differ in both emission maxima and quantum yields.

Received 3rd June 2024,
Accepted 9th July 2024

DOI: 10.1039/d4py00601a

rsc.li/polymers

Introduction

Living anionic polymerization introduced by Michael Szwarc in 1956 offers excellent control over molecular weights and the dispersity $Đ$ of polymers.[1,2] It has been widely used for the polymerization of 1,3-dienes, such as 1,3-butadiene and isoprene, to generate polydiene materials for synthetic rubber. The elastic properties of these polydienes after crosslinking notably depend on their microstructure. Therefore, the main target of early studies of anionic polymerization of 1,3-dienes was the optimization of reaction parameters (*e.g.*, initiator, solvent, further additives, and temperature) to obtain a high *cis*-1,4-content.[3]

The copolymerization of 1,3-dienes, such as 1,3-butadiene (B) and isoprene (I), with styrene (S) affords a variety of possible polymer architectures.[4,5] ABA triblock copolymers have attracted attention as thermoplastic elastomers (TPEs). This architecture relies on a flexible, low T_g polydiene midblock B (*e.g.*, polyisoprene) and two outer polystyrene A blocks that act as crosslinks after cooling and vitrification.[6] In 1966, Holden and Milkovich reported that the statistical copolymerization of isoprene and styrene in apolar solvents like cyclohexane results in block-like gradient copolymers that were later designated as "tapered".[7] The addition of a small quantity of THF with respect to the lithium-ion concentration leads to a change of the reactivity ratios and the respective monomer gradient. By varying the THF concentration, the incorporation of both monomers can be tuned to achieve ideally random incorporation, and even complete reversal of the molar composition is possible, as shown by detailed online NIR kinetics recently.[8] However, the addition of THF as a "modifier" at the same time also influences the incorporation mode of isoprene (increasing the extent of 3,4-addition) and therefore has an undesired impact on the elastic properties. As described in many studies, an increase of the number of 1,2- and 3,4-units in polydienes is observed when increasing the polarity of the system.[8–11]

Only a few studies have been reported for phenyl-substituted butadiene derivatives.[12,13] As an example, the 1-phenyl-

[a]*Department of Chemistry. Johannes Gutenberg University, Duesbergweg 10-14, 55128 Mainz, Germany. E-mail: hfrey@uni-mainz.de*
[b]*Max Planck Graduate Center, Forum Universitatis 2, 55122 Mainz, Germany*
† Electronic supplementary information (ESI) available. See DOI: https://doi.org/10.1039/d4py00601a

1,3-butadiene (PhB) monomer has been polymerized *via* either anionic or catalytic approaches.[14–17] It can be considered as a β-substituted styrene or as a 1-phenyl-substituted 1,3-butadiene.[18] This combination of two very established monomers provides an intriguing perspective. Suzuki *et al.* systematically investigated the anionic polymerization of PhB regarding its copolymerization with butadiene and styrene as well as the microstructure with respect to various parameters.[12,19–22] ^{1}H NMR studies of the resulting microstructure of PhB in different solvents revealed distinct behaviour compared to established dienes. The addition of aliquots of THF enhanced the formation of the vinylic microstructure. However, a 1,4-dominated microstructure was obtained when polymerization was performed in THF, confirmed by NMR analysis based on the chemical shifts of the aromatic protons of oligomeric structures in deuterated THF. The authors concluded that the negative charge is localized in the α-position of the phenyl ring to form the most stable anion as the active chain end. This explains why poly(1-phenyl butadiene) (PPhB) polymerized in THF shows predominantly 1,4-units.[21]

The phenyl-substituted polybutadienes showed a glass transition temperature (T_g) of around 30 °C.[17] It is worth mentioning that the T_g is in between those of the structurally similar polyisoprene ($T_g \leq -65$ °C)[23] and polystyrene (T_g = 100 °C).[11] Han *et al.* reported catalytic polymerization with a 3,4-content of 94%, resulting in a T_g of 82 °C, indicating a high dependency on the respective microstructure.[24] In a cationic polymerization approach, phenyl butadiene underwent cyclization as a side-reaction. Fundamental studies report on the targeted cationic cyclization post-polymerization of polydienes to obtain an unsaturated polycyclic species.[25–28] More recently, the cyclisation reaction was adapted to P(PhB) to maximize the T_g. Depending on the microstructure, the T_g of the cyclized material can reach nearly 200 °C, which is among the highest T_gs reported for aliphatic hydrocarbon polymers.[29] Additionally, cyclized poly(phenylbutadiene) (*cyc*P(PhB)) showed fluorescence.

Herein, we report the copolymerization of "phenyl isoprenes" with styrene and isoprene. For isoprene, the attachment of the phenyl ring can take place either at the 1- or the 4-position, resulting in a 1,2- or a 1,3-disubstituted 1,3-diene structure. While the 4-phenyl isoprene (4PhI) has been briefly described with respect to its anionic polymerization,[30] to the best of our knowledge, the 1-phenyl isoprene (1PhI) has not been employed for anionic polymerization to date. In this work, we compare 1PhI and 4PhI on a theoretical basis using density functional theory (DFT) as well as ^{13}C NMR spectroscopy to predict their reactivity in anionic polymerization. We use styrene and isoprene, respectively, for comparison. Both phenyl isoprene monomers are investigated in depth regarding their behaviour in anionic polymerization and are also copolymerized with both isoprene and styrene. For the determination of reactivity ratios, online ^{1}H NMR spectroscopy was employed. We monitored the anionic copolymerization with the structurally related monomers styrene and isoprene in cyclohexane, respectively. Finally, polymer cyclization is explored according to literature procedures, aiming at fluorescent, high T_g materials based on the reported monomers.[17,24,29,31]

Results and discussion

Synthesis of phenyl-substituted isoprene derivatives

1PhI and 4PhI were synthesized *via* a one-step Wittig reaction starting from commercially available aldehyde and ketone structures, respectively. For the synthesis of 1PhI, using the potassium *tert*-butoxide monomer, yields exceeding 75% were achieved. However, the stronger base sodium hexamethyldisilyl amine (NaHMDS) is required to achieve similar yields for the ketone benzylidene acetone. A straightforward method was established for the separation of triphenylphosphine oxide including precipitation, centrifugation and subsequential distillation. The details are given in the ESI.†

Since 1PhI and 4PhI can be viewed as β-substituted styrene derivatives, we estimate the reactivity of both monomers in analogy to previously described methods. ^{13}C NMR spectroscopy was utilized to estimate the reactivity of *para*-substituted styrene derivatives by Hirao *et al.*[32] The β-carbon shift identifies the electron charge density of the reactive vinyl bond. Increasing the polarization of the reacting carbon–carbon bond leads to increased reactivity. Therefore, it is in good agreement with the monomer reactivity in anionic polymerization. If 1PhI and 4PhI are viewed as styrene derivatives, the chemical shift of C1 as assigned in Scheme 1 was identified. Thus, 4PhI (δ = 117.45 ppm, $CDCl_3$) is expected to be much more reactive compared to styrene (δ = 113.36 ppm, $CDCl_3$), while 1PhI (δ = 113.02 ppm, $CDCl_3$) should be slightly less reactive in anionic copolymerization in apolar media.

Furthermore, DFT calculations of both monomers were conducted to obtain further theoretical insights. Fig. 1 shows the relative electron densities of both 1PhI and 4PhI in comparison with the values calculated for isoprene (differences shown in brackets). Focusing on the free methylene groups, which are most likely to be attacked by nucleophilic reagents, 4PhI (−0.176e) exhibits a lower charge at this position compared to 1PhI (−0.193e). Hence, the nucleophilic attack as part of the propagation is prone to occur, supporting the expectation based on ^{13}C NMR spectroscopy. Nevertheless, the electron densities of the reactive double bond show just a minor deviation from the 3,4-double bond in isoprene, which is

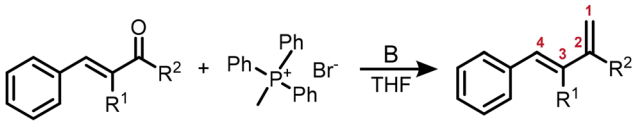

1PhI: $R^1 = CH_3$; R^2 = H; B = KO*t*Bu
4PhI: R^1 = H; $R^2 = CH_3$; B = NaHDMS

Scheme 1 Synthesis route to the phenyl-substituted isoprene derivatives.

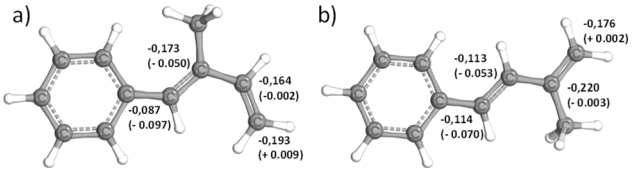

Fig. 1 3D visualization of (a) 1PhI and (b) 4PhI, respectively, with the corresponding partial charges of the dienic carbon atoms calculated using DFT. In brackets, the deviations from the calculated electron densities of isoprene are given.[59,60]

assumed to be the one reacting in the anionic polymerization. This could be interpreted in terms of a fast crossover reaction in both directions.

Homopolymerization of PhIs with *sec*-BuLi in cyclohexane

Both monomers 1PhI and 4PhI can be interpreted as a structural combination of styrene and isoprene. To investigate whether their behaviour in the anionic polymerization resembles that of S or I, a series of homopolymers with increasing M_n has been synthesized. All polymerizations were carried out in cyclohexane, using *sec*-butyl lithium as an initiator at room temperature. Subsequently, the homopolymers were characterized *via* SEC, ^{1}H NMR spectroscopy and DSC. Table 1 summarizes all characterization data of the obtained polymers, which possessed molecular weights in good agreement with the targeted values in a range of 4.6–48.8 kg mol^{-1} (SEC, eluent THF, and PS calibration) with low dispersities ($Đ \leq 1.13$). The SEC-determined molecular weights are strongly dependent on the calibration standard employed.

The microstructures of both P(1PhI) and P(4PhI) were investigated by ^{1}H NMR spectroscopy in analogy to previously reported studies.[12,17] The spectra (Fig. 2) show the olefinic signals used for the determination of the microstructures. The signals were assigned according to the reported microstructure of P(1-phenyl butadiene).[12] The sharp signals of P(4PhI) indicate a highly defined composition, which is supported by the integration, showing 94% 1,4-units. This is consistent with the microstructure of polyisoprene obtained under these conditions.[33] In comparison, the ^{1}H NMR spectrum of P(1PhI) displays broad signals with a microstructure consisting of 66% 1,2-units. This result can be explained by a sterically hindered 1,4-addition reaction, as previously suggested for 1,1-disubstituted 1,3-dienes.[34]

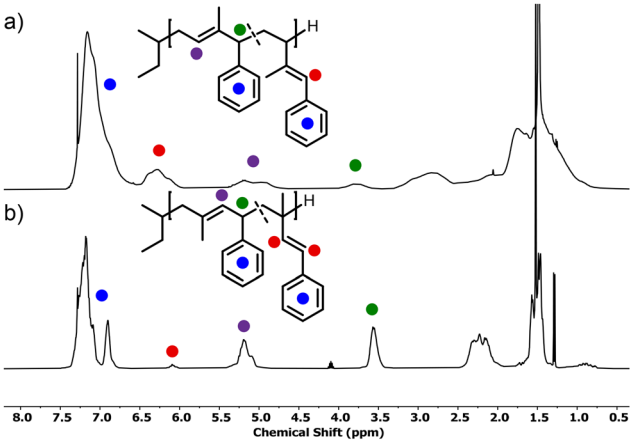

Fig. 2 ^{1}H NMR spectra ($CDCl_3$, 400 MHz) of (a) P(1PhI) and (b) P(4PhI).

The SEC traces shown in Fig. 3 confirm the good control of the polymerization for both monomers, resulting in narrow, monomodal distributions. A high degree of agreement was observed between the targeted molecular weights and the results based on PI calibration, which can be taken as an indirect confirmation of the predominant 1,4-microstructure. In contrast, the prevalence of the 1,2-microstructure in P(1PhI) samples underlines why PS calibration yields values that exhibit closer proximity to theoretical predictions.

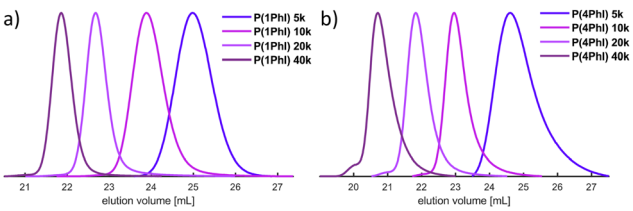

Fig. 3 SEC traces of the synthesized homopolymers with increasing targeted M_n from (a) 1-phenyl isoprene and (b) 4-phenyl isoprene.

Table 1 Overview of the homopolymers synthesized *via sec*-butyllithium initiated polymerization in cyclohexane

Entry	M	M_n^{targ} (kg mol^{-1})	$M_n{}^a$ (kg mol^{-1})	$M_n{}^b$ (kg mol^{-1})	$Đ$	1,4-PhI^c (%)	1,2-PhI^c (%)	T_g (°C)
1	1PhI	5	3.6	4.6	1.06	42	58	62
2		10	6.5	8.5	1.05	34	66	69
3		20	13.6	18.4	1.04	35	65	65
4		40	24.0	32.4	1.02	37	63	69
5	4PhI	5	3.8	4.7	1.13	85	15	47
6		10	10.7	13.6	1.07	94	6	47
7		20	22.6	30.0	1.09	94	6	48
8		40	48.8	64.8	1.11	94	6	48

^{a} Determined by SEC (THF, PI calibration, and RI detector). ^{b} Determined by SEC (THF, PS calibration, and RI detector). ^{c} Determined from the olefinic region of the ^{1}H NMR spectra (400 MHz, $CDCl_3$).

Addition of polar additives

The polymerization of 1,3-dienes is known to depend on several parameters (*e.g.*, chain end and monomer concentration, temperature, solvent, *etc.*) in terms of the regio-isomeric composition of the resulting polymers.[8,35–38] The polarity of the solvent is a key parameter, since it determines the coordination of the chain end to the lithium ion.[39] In numerous studies, it was shown that the addition of aliquots of THF in the polymerization of 1,3-dienes increases the content of vinylic units.[8,9,40] Furthermore, the addition of THF accelerates propagation kinetics. This effect has been observed in both isoprene and styrene, where propagation reaches a maximum before further addition of THF decelerates propagation.[41,42]

For 1-phenyl butadiene, it was reported that upon addition of a few aliquots of THF, the ratio of 1,2-units increases.[12] Further increasing the content of THF and polymerization in pure THF led to a maximum of 90% 1,4-content. In a similar fashion, we conducted the polymerization of 1PhI and 4PhI in cyclohexane with 2 and 20 equivalents of THF with respect to the lithium-ion concentration. Furthermore, we carried out the polymerization reaction in pure THF at −78 °C. It should be noted that common dienes, such as myrcene and isoprene, are not capable of polymerizing under these conditions.[43,44] As listed in Table 2, the addition of THF has an impact on the resulting microstructure as the ratio of vinyl units increases. In line with previous observations for PhB, in pure THF, more than 80% 1,4-units were formed. A tentative explanation might be given by the reactivity of the chain end and the resulting propagation rates. Strohmann *et al.* reported experiments with *tert*-butyl lithium and THF in a ratio of 1 : 2, revealing remarkable aggregation, leading to an increase in reactivity compared to the ratios 1 : 1 and 1 : 2.5.[45] Consequently, the polymerization rate is enhanced by small amounts of THF, promoting the formation of vinylic units. The faster kinetics may also explain the broad distribution observed for entry 12. Carrying out the polymerization of 4PhI with 2 equivalents of THF with respect to the BuLi concentration did not result in dispersities lower than 1.4, as illustrated in Fig. S16.† Further increasing the polarity supports the formation of the most stable anion. For both 1PhI and 4PhI, the charge will be delocalized in the aromatic ring as demonstrated for PhB.[21,22] Therefore, one observes the predominant formation of 1,4-units with increasing polarity of the system, as obvious from a comparison of the respective ^{1}H NMR spectra (Fig. 4).

As expected, DSC measurements of the resulting polymers show a clear correlation between the glass transition and the respective microstructure. For example, 1PhI polymerized in THF with a high 1,4-content exhibited a lower T_g of 50 °C compared to 67 °C when polymerized in cyclohexane due to its more flexible backbone compared to P1PhI synthesized in cyclohexane, which is dominated by a 1,2-microstructure (Fig. S14†). As shown by the values in Table 2, the T_gs for the P1PhI samples prepared in different systems shift to higher temperature with increasing solvent polarity. P4PhI polymerized in either cyclohexane or THF always resulted in a high 1,4-content. Therefore, as shown in Fig. S15,† the T_gs of both samples are in the same range of 50–56 °C. A higher 1,2-content can raise the T_g to 73 °C.

In situ ^{1}H NMR: copolymerisation with styrene as a comonomer

Living poly(1PhB) chain ends were not sufficiently reactive to initiate the polymerization of butadiene or styrene in THF. Reaching a maximum of 35% block efficiency, only bimodal

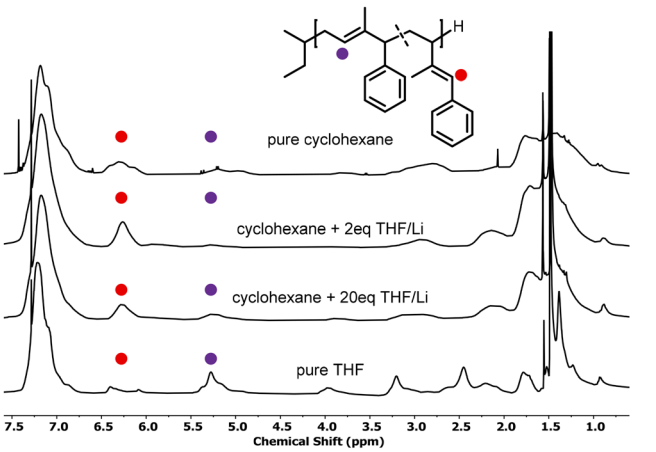

Fig. 4 Stacked ^{1}H NMR spectra of P(1PhI) polymerized with increasing concentrations of THF, resulting in microstructures with shifting ratios.

Table 2 Data of the polymer samples obtained when investigating the impact of THF on the polymerization of PhI monomers in cyclohexane

Entry	M	M_n^{targ} (kg mol^{-1})	M_n[b] (kg mol^{-1})	$\frac{[THF]}{[Li]}$	$Đ$	1,4-PhI[c] (%)	1,2-PhI[c] (%)	T_g (°C)
1	1PhI	10	7.8	0	1.05	34	66	67
9		10	10.3	2	1.07	12	88	62
10		10	11.1	20	1.08	33	67	53
11[a]		10	9.6	Pure	1.06	85	15	50
5	4PhI	10	13.9	0	1.09	94	6	56
12		10	7.1	2	1.44	n.d.	n.d.	73
13		10	8.7	20	1.15	56	44	63
14[a]		10	9.9	Pure	1.08	82	18	50

[a] Polymerization at −78 °C. [b] Determined by SEC (THF, PS calibration, and RI detector). [c] Calculation using the respective olefinic signals of the ^{1}H NMR spectra.

distributions were reported. However, reverse monomer addition resulted in monomodal SEC traces, confirming that all living chain ends initiated 1PhB.[20]

To investigate the statistical copolymerization behaviour of both monomers with styrene and isoprene, respectively, we conducted real-time ^{1}H NMR spectroscopy to evaluate the reactivity ratios. First, copolymerization reactions of styrene with 1PhI and 4PhI, respectively, were conducted. During the statistical copolymerization, individual monomer peaks were traced to determine monomer conversion. Due to the absence of termination and transfer reactions in classical anionic polymerization, monitoring of the integrals can also be used to determine the relative position along the growing chains.[46,47] The stacked ^{1}H NMR spectra for the copolymerization of styrene and 1PhI are shown in Fig. 5 and in Fig. S18† for 4PhI. The monomer concentrations plotted as a function of time and total conversion, respectively, show preferential consumption of the phenyl isoprenes over styrene in both cases.

The collected data were used to calculate the reactivity ratios r_{PhI} and r_S, as listed in Table 3. They define the ratio between the rate of homopolymerization and the rate of the crossover reaction. Using the non-terminal model of Jaacks, the values were determined.[48] Based on these evaluated parameters, plots of the relative comonomer position along the chain were generated. As illustrated in Fig. 6(b) and (c), for both systems, a pronounced gradient is observed. The steeper gradient for the 4PhI system confirms 4PhI to be more reactive, supporting the hypothesis derived from the β-C-shift.

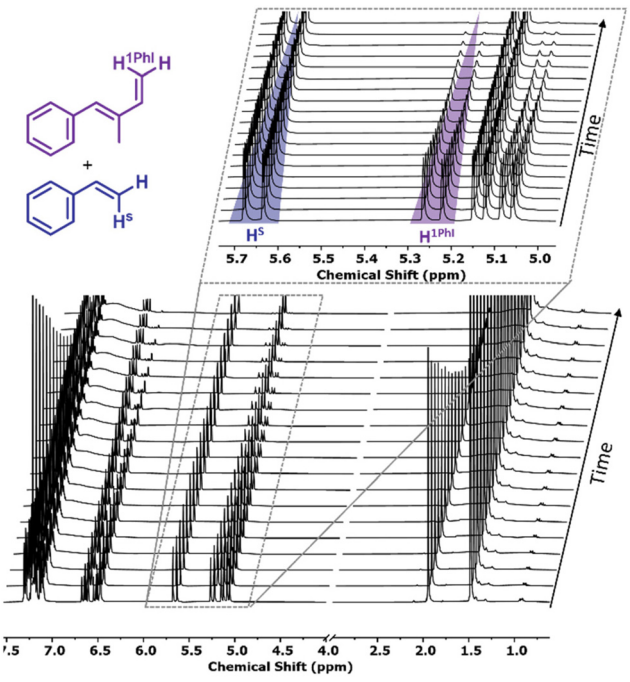

Fig. 5 Stacked ^{1}H NMR spectra (400 MHz, C_6D_{12}) of the copolymerization of styrene/1PhI as a function of time. The zoomed-in region shows the peaks tracked for the evaluation of the respective comonomer consumption.

Table 3 Evaluated reactivity ratios of the copolymerization of styrene with 1PhI and 4PhI, respectively, using the Jaacks model. For comparison, the reactivity ratios of dienes and styrene are given as well

Diene	r_{diene}	r_S
1-Phenyl isoprene	3.38	0.30
4-Phenyl isoprene	9.20	0.109
Isoprene[49]	11	0.049
β-Myrcene[50]	36	0.028
β-Farnesene[51]	27	0.037
cis-Ocimene[52]	1.015	0.985
trans-Ocimene[52]	0.62	1.52
Vinylcyclohexene[53]	0.39	2.56

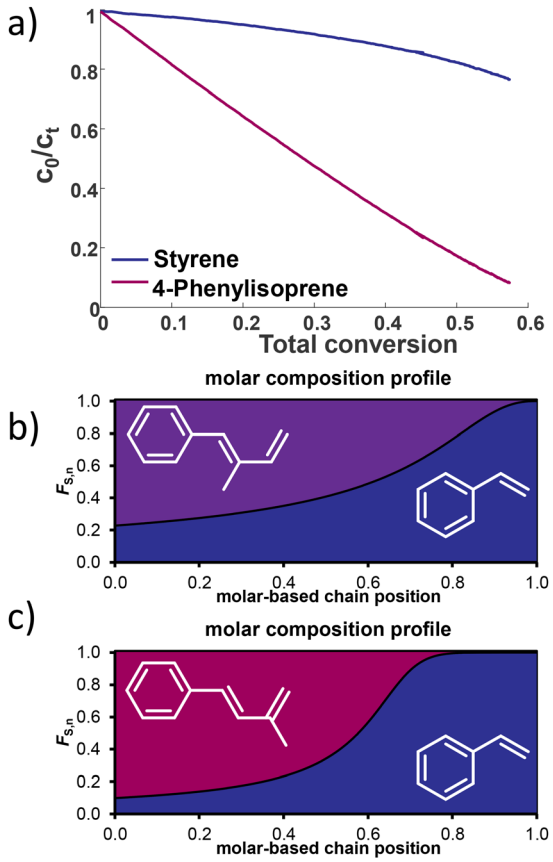

Fig. 6 (a) Monomer conversion for the copolymerization of S and 4PhI. Calculated molar composition profiles of S and (b) 1PhI and (c) 4PhI, respectively.

However, in contrast to the abovementioned assumption, 1PhI is also consumed faster, although the carbon shift indicated the opposite. This demonstrates that these simple considerations cannot be applied to diene systems. Reactivity ratios calculated using the terminal model of the Meyer–Lowry fit are given in the ESI.†

In comparison with the reactivity ratios observed for the copolymerization of styrene with isoprene (substituted in the 2-position) and myrcene (Table 3), the di-substituted 1PhI and 4PhI display a less pronounced gradient. Nevertheless, it is

worth noting that the 1,2-disubstituted 1PhI demonstrates higher reactivity ratios compared to previously reported 1,2-disubstituted dienes (*i.e.*, *trans*- and *cis*-ocimene and 1-vinyl cyclohexene).[52,53] To the best of our knowledge, 4PhI is the first 1,3-disubstituted 1,3-diene that has been investigated regarding its copolymerization kinetics with styrene.

In situ ^{1}H NMR kinetics with isoprene as a comonomer

In analogy to the investigation of copolymerization with styrene, we also studied *in situ* ^{1}H NMR kinetics for copolymerization with isoprene (I). Due to the diene nature of both monomers, the respective peaks overlapped, as shown in the stacked spectra as a function of time in Fig. S21 and S22.† From the obtained data, the plots of the comonomer concentrations *vs*. the total conversion and against time are given in Fig. 7 and in the ESI.† To our surprise, the copolymerization of 4PhI with I did not result in plausible results, neither for the Jaacks nor for the Meyer–Lowry fit, when carried out in an equimolar ratio. Repeating the copolymerization under the same conditions or with a ratio of 70 : 30 did not improve the given results, which are illustrated in the ESI.† Using the Meyer–Lowry fit, in all cases the reactivity ratios were calculated to exceed 1, as summarized in Table S3.† In comparison, the obtained data do not reflect the theoretical Jaacks fit. Nevertheless, the stacked NMR spectra in Fig. S22† indicate a faster consumption of isoprene compared to 4PhI.

The Jaacks fit was successfully used for 1PhI and isoprene, confirming the almost ideally random copolymerization with reactivity ratios of r_I = 1.155 and r_{1PhI} = 0.865. The cross-over reaction seems to be independent of the monomer. This might be explained by the similar electron densities calculated using DFT. A comparison with the known reactivity ratios using myrcene as another diene is given in Table 4.

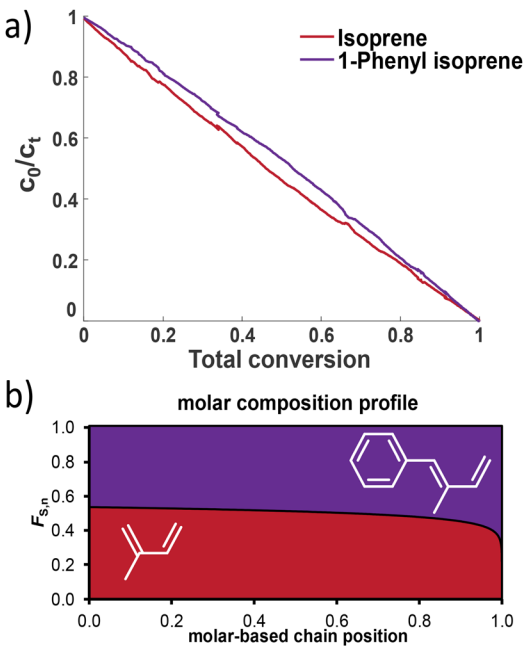

Fig. 7 (a) Monomer conversion in the copolymerization of I and 1PhI and (b) the molar composition profile of the copolymer of I and 1PhI.

Table 4 Reactivity ratios of the copolymerization of isoprene and reported 1,3-dienes

Monomer A	r_A	r_I
1PhI	0.865	1.155
4PhI	n.d.	n.d.
β-Myrcene[50]	4.4	0.23

Copolymerization with isoprene and styrene

The determined reactivity ratios may lead to unique material properties. Therefore, the copolymerizations were conducted on a larger scale (Fig. 8). A rather high molecular weight of 40 kg mol^{-1} was targeted to induce phase separation despite the gradient structure (Table 5). In all cases, monomodal distributions with a low dispersity ($Đ$ < 1.11) were obtained. The stacked ^{1}H NMR spectra in Fig. S28† show the characteristic signals of the monomers. The gradient structure in the anionic copolymerization of I and S can be visually tracked through the gradual colour change with monomer conversion. This results in a decreasing concentration of the colorless polydienyl chain ends and a gradually increasing concentration of orange polystyryl chain ends. For both copolymerization reactions with isoprene, an immediate coloration of the solution was observed after initiation. Throughout the polymerization, no colour change was observed. Therefore, as shown before, a significant number of polyphenylisoprenyl chain ends were present from the beginning. To lend further support to the completely random distribution of 1PhI throughout the chain when copolymerized with isoprene, we observed only one glass transition at 3 °C. The copolymer P(I-*co*-4PhI) exhibits a broad softening regime rather than a defined glass transition.

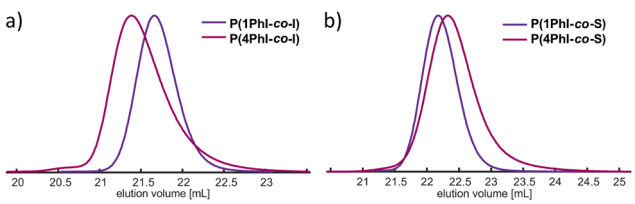

Fig. 8 SEC traces of the copolymerization of 1PhI and 4PhI with (a) isoprene and (b) styrene.

Table 5 Summarized data of the copolymerization of phenyl isoprenes with isoprene or styrene as a comonomer

Entry	Monomer (A)	Monomer (B)	M_n^{targ} (kg mol^{-1})	$M_{n,SEC}$[a] (kg mol^{-1})	$Đ$	T_g (°C)
15	1PhI	I	40	33.8	1.04	3
16	1PhI	S	40	35.6	1.05	67
17	4PhI	I	40	37.9	1.09	−10
18	4PhI	S	40	29.7	1.11	61

[a] Determined by SEC (THF, PS calibration, and RI detector).

Further drying in a high vacuum and the change of the heating rate did not clarify the inflection point. The soft gradients of the styrenic copolymers prevented phase segregation, resulting in merely one T_g >60 °C.

Cyclization to enhance thermal properties and prepare fluorescent materials

The synthesized homopolymers show lower T_gs compared to polystyrene (T_g = 100 °C).[11] However, since the phenyl rings are all adjacent to double bonds, cationic cyclization can be performed to alter the thermal properties. As already presented for butadiene-derived structures, the trifluoromethanesulfonic acid-initiated modification influences the thermal properties of these polymers drastically.[16,17,24,29,31,54–56] Consequently, the cyclized P(PhI) structures are expected to exhibit strongly increased rigidity and thus high T_g values. The selected polymers (entries 4 and 8 of Table 1) with a targeted molecular weight of 40 kg mol^{-1} were cyclized using CF_3SO_3H in cyclohexane at room temperature (Scheme 2). After drying, amber-coloured powders were obtained. Since the samples remained soluble in a variety of solvents after the intramolecular cyclization, they were investigated by SEC and NMR analyses. The SEC traces shown in Fig. 9 and S33† present the expected shift to a higher elution volume. The SEC traces (Fig. S33†) show a signal for the flow rate marker toluene, indicating the presence of a polymer rather than degradation to small molecules. This discovery was described by Han *et al.* and attributed to the compression of the polymer chain and an increase in hydrodynamic radii.[29] DSC measurements verified the expected increase of the T_g values (Table 6). The cyclization effect on the T_g values is stronger for *cyc*P(1PhI), with T_g reaching 180 °C after cyclization. The T_g of *cyc*P(4PhI) was determined to be 131 °C.

In agreement with the reported *cyc*P(PhB) of Ma and coworkers, we observed that the cyclized P(PhI) samples show fluorescence when irradiated with UV light (Fig. 9).[17] This observation is most likely explained by a clusterization-trig-

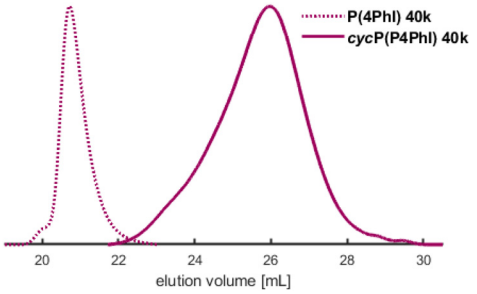

Fig. 9 SEC traces of the cyclized P4PhI in comparison with the initial polymer (entry 8, Table 1).

Table 6 Summarized data of the changed material properties after the cyclization reaction

Entry	Entry of the precursor	Polymer	M_n[a] (kg mol^{-1})	$Đ$	T_g (°C)
19	4	P1PhI	3.2	1.63	187
20	8	P4PhI	2.9	1.45	131

[a] Determined by SEC (THF, PS calibration, and RI detector).

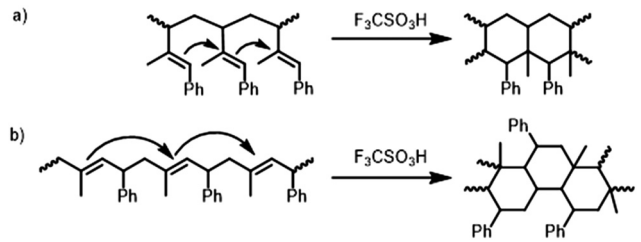

Scheme 2 Proposed mechanism for the cyclization of the predominant microstructures of (a) P1PhI and (b) P4PhI in analogy to the literature.[24]

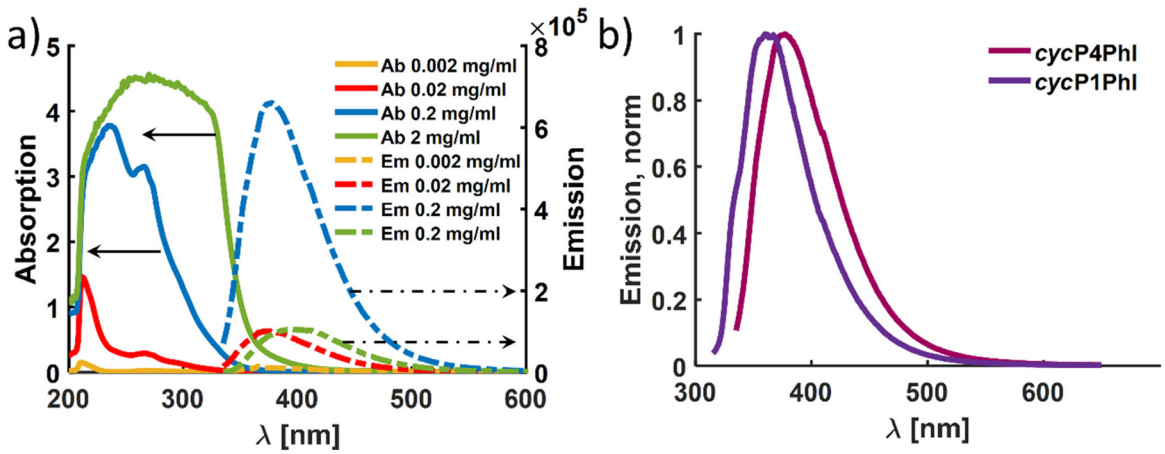

Fig. 10 (a) Absorption (solid) and emission (dashed) spectra of cyclized P4PhI at different concentrations in toluene (λ_{exc} = 330 nm) and (b) normalized emission spectra of *cyc*P1PhI and *cyc*P4PhI in toluene (c = 0.2 mg mL^{-1}, $\lambda_{exc,cycP1PhI}$ = 310 nm and $\lambda_{exc,cycP4PhI}$ = 330 nm).

gered emission.[57] To quantify the photochemical properties dependent on presumed clusterization, absorption and emission properties were determined using four different concentrations (2, 0.2, 0.02, and 0.002 mg mL^{-1}). The main questions raised were (i) whether the introduction of the methyl group leads to a shift in the emission maximum compared to the *cyc*P(PhB) polymer due to different ordering and (ii) whether the differing initial microstructures of P1PhI and P4PhI might result in distinct emission properties. In Fig. 10a, the emission spectra of the solutions of *cyc*P(P4PhI) with decreasing dilution are shown (λ_{exc} = 330 nm). Due to the high optical density and therefore self-absorption, the sample with the highest concentration shows a significantly reduced emission intensity compared to the other concentrations under the same conditions. At the same time, the emission maximum shifts from 375 nm to 395 nm (Table S4†). In contrast to previously reported interpretation clusterization-triggered emission,[57] we propose that the emission maximum shifts apparently and its intensity decreases due to inner filter effects with increasing concentration. Going from *cyc*P1PhI to *cyc*P4PhI, a presumed impact of the initial microstructure is observable with the emission maximum shifting from 360 nm to 377 nm (Fig. 10b). The absolute quantum yields of both samples in the solid state were determined using an integrating sphere. In both cases, the observed self-absorption decreases the overall quantum yield. As it is higher for *cyc*P4PhI (4.1%) than for *cyc*P1PhI (2.9%), *cyc*P4PhI is a more efficient candidate for utilization in organic light-emitting diodes (OLEDs).

Experimental

Terminology

(*E*)-(2-Methylbuta-1,3-dien-1-yl)benzene and (*E*)-(3-methylbuta-1,3-dien-1-yl)benzene are abbreviated as 1PhI and 4PhI, respectively.

Instrumentation

SEC measurements were performed using an Agilent 1100 Series system equipped with a SDV column set from PSS (SDV 103, SDV 105, and SDV 106). Tetrahydrofuran (THF) was used as the mobile phase (flow rate: 1 mL min^{-1}) and as the solvent. The calibration standards polystyrene and polyisoprene were provided by PSS. Measurements were performed at 30 °C with both RI and UV (275 nm) detectors and toluene was used as a reference. The data analysis was carried out using PSS WinGPC UniChrom (V 8.31, Build 8417) software provided by PSS Polymer Standards Service GmbH. NMR spectra were recorded on a Bruker Avance 400 spectrometer at 400 MHz for ^{1}H NMR and 103 MHz for ^{13}C NMR. The determination of glass transition temperatures (T_g) was performed on a DSC 250 (TA Instruments) differential scanning calorimeter. Two heating cycles and one cooling cycle were conducted at a rate of 10 °C min^{-1}. A detailed description of the DSC measurements and the description of the photochemical measurements are given in the ESI.†

Monomer and polymer synthesis

Both novel monomers 1PhI and 4PhI were synthesized in a one-step Wittig reaction. Alterations to published procedures are given in the ESI† together with a detailed description of the polymerization conditions.

Real-time ^{1}H NMR

The measurements were conducted on a 400 MHz Bruker Avance spectrometer. All spectra are referenced internally to the residual proton signal of deuterated cyclohexane-d_{12}. The polymerization mixtures were prepared in an argon-filled glove box. Monomers and solvents were purified over calcium hydride and trioctyl aluminum in the case of the monomers. The measurements were performed in a conventional NMR tube sealed with a rubber septum.

Prior to initiation, a first spectrum was recorded and equilibrated to a temperature of 25 °C. Following the initiation using 30 μL of *sec*-butyl lithium (0.65 M in cyclohexane), the NMR experiment was started, in which every 30 s, a scan was performed over a period of 6 to 7 hours. By tracking the decrease of the respective monomer signals, determination of the reactivity ratios was achieved using NIREVAL software designed by our group.[58]

Cyclization

The cyclization reaction was performed according to the literature. Into a solution of 200 mg P(4PhI) dissolved in 25 mL cyclohexane, trifluorosulfonic acid (0.2 mL, 2 eq. per double bond in every repeating unit) was added. The dark solution was quenched after 1 hour using a 1 wt% aqueous sodium carbonate solution. After washing with water, the polymer was precipitated in methanol and dried under vacuum.

Conclusion

In this work, the anionic polymerization of two isoprene derivatives, *i.e.*, 1-phenyl isoprene and 4-phenyl isoprene, was introduced. 4PhI was investigated in more detail than in earlier reports, and 1PhI has not been described to date. The difference in the substitution pattern of 1,3-dienes was expected to result in different reactivities, as already indicated by their β-C-shifts and by DFT calculations. Butyl lithium-initiated polymerizations allowed for the synthesis of polymers with narrow molar mass distributions and good control over the molecular weights in a range of 4.6 to 48.8 kg mol^{-1}. ^{1}H NMR spectroscopy revealed the expected differences in the microstructures. This was further modified using THF, leading to unusual behaviour caused by the attached phenyl ring. Online NMR kinetics uncovered a preference for the phenyl-substituted isoprene over styrene, despite the initial theoretical results predicting reduced reactivity of 1PhI. Nevertheless, these predictions are in line with the data obtained from kinetics with isoprene, which showed random incorporation for 1PhI/I. DSC measurements of the respective compositions further revealed merely one glass transition. In a post-polymer-

ization cyclization reaction, soluble materials with distinct photophysical properties were obtained. The characterization revealed an apparent dependency of the fluorescence maximum on the different microstructures of the starting materials due to self-absorption. As those materials also present a pronounced increase in rigidity, as indicated by the drastic increase of the glass transition temperature, they could be considered intriguing building blocks for block copolymers with an intramolecularly crosslinked high T_g block.

Author contributions

Moritz Rauschenbach: conceptualization, data curation, investigation, methodology, validation, visualization, and writing. Gregor Linden, Ramona Barent, and Laura Stein: investigation, data curation, and methodology. Holger Frey: conceptualization, supervision, and writing – review and editing.

Data availability

The data supporting this article have been included as part of the ESI.†

Conflicts of interest

There are no conflicts to declare.

Acknowledgements

The authors acknowledge A. H. E. Müller for valuable discussions and for critically reviewing the results of the online NMR kinetics. We thank the Deutsche Forschungsgemeinschaft DFG for funding *via* INST 247/1018-1 FUGG to Katja Heinze.

References

1 M. Szwarc, *Nature*, 1956, **178**, 1168–1169.
2 A. Hirao, R. Goseki and T. Ishizone, *Macromolecules*, 2014, **47**, 1883–1905.
3 N. Hadjichristidis and A. Hirao, *Anionic Polymerization*, Springer, Tokio, 2013.
4 F. S. Bates, M. A. Hillmyer, T. P. Lodge, C. M. Bates, K. T. Delaney and G. H. Fredrickson, *Science*, 2012, **336**, 434–440.
5 K. Ntetsikas, V. Ladelta, S. Bhaumik and N. Hadjichristidis, *ACS Polym. Au*, 2022, **3**, 158–181.
6 W. Wang, W. Lu, A. Goodwin, H. Wang, P. Yin, N. G. Kang, K. Hong and J. W. Mays, *Prog. Polym. Sci.*, 2019, **95**, 1–31.
7 G. Holden and R. Milkovich, US Patent 3265765, 1966.
8 M. Steube, T. Johann, H. Hübner, M. Koch, T. Dinh, M. Gallei, G. Floudas, H. Frey and A. H. E. Müller, *Macromolecules*, 2020, **53**, 5512–5527.
9 D. A. H. Fuchs, H. Hübner, T. Kraus, B. J. Niebuur, M. Gallei, H. Frey and A. H. E. Müller, *Polym. Chem.*, 2021, **12**, 4632–4642.
10 L. Shaw and L. R. Hutchings, *Polym. Chem.*, 2020, **11**, 7020–7025.
11 A. H. E. Müller and K. Matyjaszewski, *Controlled and Living Polymerizations: From Mechanisms to Applications*, Wiley-VCH Verlag, Weinheim, 2010.
12 T. Suzuki, Y. Tsuji and Y. Takegami, *Macromolecules*, 1978, **11**, 639.
13 T. Suzuki, Y. Tsuji, Y. Takegami and H. J. Harwood, *Macromolecules*, 1979, **12**, 234.
14 S. Pragliola, M. Cipriano, A. C. Boccia and P. Longo, *Macromol. Rapid Commun.*, 2002, **23**, 356–361.
15 J. Lin, F. Wang, C. Zhang, H. Liu, D. Li and X. Zhang, *RSC Adv.*, 2021, **11**, 23184–23191.
16 Y. Jiang, X. Kang, Z. Zhang, S. Li and D. Cui, *ACS Catal.*, 2020, **10**, 5223–5229.
17 H. Bai, L. Han, W. Li, C. Li, S. Zhang, X. Wang, Y. Yin, H. Yan and H. Ma, *Macromolecules*, 2021, **54**, 1183–1191.
18 Y. Qi, Z. Liu, S. Liu, L. Cui, Q. Dai, J. He, W. Dong and C. Bai, *Catalysts*, 2019, **9**, 97.
19 T. Suzuki, Y. Tsuji, Y. Watanabe and Y. Takegami, *Macromolecules*, 1980, **13**, 849–852.
20 Y. Tsuji, T. Suzuki, Y. Watanabe and Y. Takegami, *Macromolecules*, 1981, **14**, 1194–1196.
21 T. Suzuki, Y. Tsuji, Y. Watanabe and Y. Takegami, *Polym. J.*, 1979, **11**, 651–660.
22 Y. Tsuji, T. Suzuki, Y. Watanabe and Y. Takegami, *Polym. J.*, 1981, **13**, 1099–1110.
23 J. M. Widmaier and G. C. Meyer, *Macromolecules*, 1981, **14**, 450–452.
24 Y. Cai, J. Lu, D. Zuo, S. Li, D. Cui, B. Han and W. Yang, *Macromol. Rapid Commun.*, 2018, **39**, 1800298.
25 R. K. Agnihotri, D. Falcon and E. C. Fredericks, *J. Polym. Sci., Part A-1: Polym. Chem.*, 1972, **10**, 1839–1850.
26 A. Priola, M. Bruzzone, F. Mistrali and S. Cesca, *Angew. Makromol. Chem.*, 1980, **88**, 1–19.
27 R. Y. Asami, K.-I. Hasegawa and T. Onoe, *Polym. J*, 1976, **8**, 43–52.
28 J. Lal, *Polymer*, 1998, **39**, 6183–6186.
29 Y. Cai, J. Lu, G. Jing, W. Yang and B. Han, *Macromolecules*, 2017, **50**, 7498–7508.
30 J. Li and J. He, *ACS Macro Lett.*, 2015, **4**, 372–376.
31 Q. Lv, C. K. Yu, Q. Yin, J. Lu and B. Han, *J. Macromol. Sci., Part A: Pure Appl.Chem*, 2020, **57**, 388–397.
32 T. Ishizone, A. Hirao and S. Nakahama, *Macromolecules*, 1993, **26**, 6964–6975.
33 H. Hsieh and R. Quirk, *Anionic polymerization: principles and practical applications*, Dekker, New York, 1996.
34 S. Uchida, K. Togii, S. Miyai, R. Goseki and T. Ishizone, *Macromolecules*, 2020, **53**, 10107–10116.
35 A. Forens, K. Roos, C. Dire, B. Gadenne and S. Carlotti, *Polymer*, 2018, **153**, 103–122.

36 T. A. Antkowiak, A. E. Oberster, A. F. Halasa and D. P. Tate, *J. Polym. Sci., Part A-1: Polym. Chem.*, 1972, **10**, 1319–1334.
37 W. Gebert, J. Hinz and H. Sinn, *Makromol. Chem.*, 1971, **144**, 97–115.
38 D. J. Worsfold and S. Bywater, *Macromolecules*, 1978, **11**, 582–586.
39 H. Hsieh, D. J. Kelley and A. V. Tobolsky, *J. Polym. Sci.*, 1957, **26**, 240–242.
40 C. A. Uraneck, *J. Polym. Sci., Part A-1: Polym. Chem.*, 1971, **9**, 2273–2281.
41 S. Bywater and D. J. Worsfold, *Can. J. Chem.*, 1962, **40**, 1564–1570.
42 M. Morton and L. J. Fetters, *J. Polym. Sci., Part A: Gen. Pap.*, 1964, **2**, 3311–3326.
43 J. Bareuther, M. Plank, B. Kuttich, T. Kraus, H. Frey and M. Gallei, *Macromol. Rapid Commun.*, 2021, **42**, 2000513.
44 A. Garton, R. P. Chaplint and S. Bywater, *Eur. Polym. J.*, 1976, **12**, 697–700.
45 J. Kleinheider, T. Schrimpf, R. Scheel, T. Mairath, A. Hermann, K. Knepper and C. Strohmann, *Chem. – Eur. J.*, 2024, **30**, e202304226.
46 A. Natalello, M. Werre, A. Alkan and H. Frey, *Macromolecules*, 2013, **46**, 8467–8471.
47 T. Johann, D. Leibig, E. Grune, A. H. E. Müller and H. Frey, *Macromolecules*, 2019, **52**, 4545–4554.
48 V. Jaacks, *Makromol. Chem.*, 1972, **161**, 161–172.
49 S. P. Wadgaonkar, M. Wagner, L. A. Baptista, R. Cortes-Huerto, H. Frey and A. H. E. Müller, *Macromolecules*, 2023, **56**, 664–677.
50 C. Hahn, M. Rauschenbach and H. Frey, *Angew. Chem., Int. Ed.*, 2023, **62**, e202302907.
51 E. Grune, T. Johann, M. Appold, C. Wahlen, J. Blankenburg, D. Leibig, A. H. E. Müller, M. Gallei and H. Frey, *Macromolecules*, 2018, **51**, 3527–3537.
52 E. Grune, J. Bareuther, J. Blankenburg, M. Appold, L. Shaw, A. H. E. Müller, G. Floudas, L. R. Hutchings, M. Gallei and H. Frey, *Polym. Chem.*, 2019, **10**, 1213–1220.
53 C. Wahlen, J. Blankenburg, P. Von Tiedemann, J. Ewald, P. Sajkiewicz, A. H. E. Müller, G. Floudas and H. Frey, *Macromolecules*, 2020, **53**, 10397–10408.
54 K. Liu, F. Zhang, M. Sun, F. Xie, S. Ying, Z. Yang, C. Zhou, J. Xia, A. Li, K. Liu, F. Zhang, M. Sun, F. Xie, S. Ying, Z. Yang, C. Zhou, J. Xia and A. Li, *Macromol. Chem. Phys.*, 2020, **221**, 2000161.
55 A. Nakahara, K. Satoh and M. Kamigaito, *Macromolecules*, 2009, **42**, 620–625.
56 A. Nakahara, K. Satoh, H. Saito and M. Kamigaito, *J. Polym. Sci., Part A: Polym. Chem.*, 2012, **50**, 1298–1307.
57 H. Zhang, Z. Zhao, P. R. McGonigal, R. Ye, S. Liu, J. W. Y. Lam, R. T. K. Kwok, W. Z. Yuan, J. Xie, A. L. Rogach and B. Z. Tang, *Mater. Today*, 2020, **32**, 275–292.
58 M. Steube, T. Johann, M. Plank, S. Tjaberings, A. H. Gröschel, M. Gallei, H. Frey and A. H. E. Müller, *Macromolecules*, 2019, **52**, 9299–9310.
59 A. E. Reed, R. B. Weinstock and F. Weinhold, *J. Chem. Phys.*, 1998, **83**, 735.
60 T. Y. Nikolaienko, L. A. Bulavin and D. M. Hovorun, *Comput. Theor. Chem.*, 2014, **1050**, 15–22.